

# Precise-Control Synthesis of $\alpha$ -/ $\beta$ -MnO<sub>2</sub> Materials by Adding Zn(acac)<sub>2</sub> as a Phase Transformation-Inducing Agent and Their ORR Performance

**Ningqiang Zhang,<sup>a</sup> Lingcong Li,<sup>a</sup> Guizhen Zhang,<sup>a\*</sup> Hong He<sup>a, b,\*</sup>**

<sup>a</sup>Key Laboratory of Catalysis Chemistry and Nanoscience, Department of Chemistry and Chemical Engineering, College of Environmental and Energy Engineering, Beijing University of Technology, Beijing 100124, China

<sup>b</sup>Collaborative Innovation Center of Electric Vehicles in Beijing, Beijing 100081, China

\*Corresponding author: +86-13269365626, [zhangguizhen@bjut.edu.cn](mailto:zhangguizhen@bjut.edu.cn); +86-13501149256, [hehong@bjut.edu.cn](mailto:hehong@bjut.edu.cn).

**Abstract:** In this paper, we present an approach for the precise-control phase transformation of MnO<sub>2</sub> to synthesis of different compositions of  $\alpha$ -/ $\beta$ -MnO<sub>2</sub> materials by adding a trace Zn(acac)<sub>2</sub> as the phase transformation-inducing agent in a hydrothermal reaction. The single-atomic dispersion of Zn might reduce the barrier of phase transformation of  $\delta$ -MnO<sub>2</sub> to  $\beta$ -MnO<sub>2</sub>. The ratio of Zn species present in single-atomic dispersion and nanoclusters might dominated the generations of  $\alpha$ -MnO<sub>2</sub> and  $\beta$ -MnO<sub>2</sub>. The oxygen reduction reaction results indicated the MnO<sub>2</sub> materials have potential applications values as promising catalysts in electrochemical catalysis.

**Keywords:**  $\alpha$ -/ $\beta$ -MnO<sub>2</sub>, phase transformation-inducing agent, oxygen reduction reaction.

## 1. Introduction (11-point boldface)

Many types of synthetic techniques have been developed in the last decade to obtain MnO<sub>2</sub> with precise phase and tunnels to control the material properties.<sup>1</sup> However, because of different types of MnO<sub>2</sub>, phase transformation of MnO<sub>2</sub> usually occurs in the process of hydrothermal synthesis of MnO<sub>2</sub> polymorphs when chalcogen elements or metal ions are introduced to reduce KMnO<sub>4</sub> to MnO<sub>2</sub> nanostructures. However, it is very difficult to obtain the precise phase content of MnO<sub>2</sub> materials because of the complexity of phase transformation process. Moreover, the synthesised products often contain significant amounts of cations, chalcogenide, and protons. Hence, the additive in hydrothermal synthesis is the key factor to control the phase transformation process, precisely controlling the phase content of MnO<sub>2</sub>.<sup>2</sup> Although a polymorph of MnO<sub>2</sub> with the same phase could be obtained, when the doping ions were introduced into the lattice or tunnel of MnO<sub>2</sub>, the properties of MnO<sub>2</sub> changed. Therefore, it is important to control the amount of doping ions because the intrinsic property of MnO<sub>2</sub> can be affected by adding a large amount of ions.

## 2. Experimental (or Theoretical)

In a typical procedure for the synthesis of mixed-MnO<sub>2</sub>, an aqueous solution (75 mL) containing MnSO<sub>4</sub>·H<sub>2</sub>O (2.4840 g), KMnO<sub>4</sub> (1.6590 g), and desired amounts of Zn(acac)<sub>2</sub> (The Zn(acac)<sub>2</sub> was weighed using a thermogravimetric microbalance with a precision of 0.0001 mg) were put into a 100 mL Teflon-lined stainless steel autoclave, and then it was sealed, and maintained at 160 °C for 24 h. The resulting black slurries were filtered, washed with deionized water for four times, and then dried at 110 °C for 24 h. All the samples were calcined at 500 °C in air for 6 h before use.

## 3. Results and discussion

The Rietveld refined XRD patterns of the five MnO<sub>2</sub> samples are shown in Fig. S1 (for details, see ESI). The XRD patterns and phase composition of  $\beta$ -MnO<sub>2</sub> are shown in Fig. 1. Without Zn(acac)<sub>2</sub>, the sample (Fig. 1B-a) can be indexed to a pure tetragonal phase [space group: I4/m (87)] of  $\alpha$ -MnO<sub>2</sub> with lattice constants  $a = 9.7847 \text{ \AA}$  and  $c = 2.8630 \text{ \AA}$  (JCPDS 44-0141). Fig. 1B shows the XRD pattern of the mixed-MnO<sub>2</sub>:  $\alpha$ -MnO<sub>2</sub> was transformed to  $\beta$ -MnO<sub>2</sub>, and also the  $\beta$ -MnO<sub>2</sub> returned the original phase ( $\alpha$ -MnO<sub>2</sub>) with the increase in the amount of Zn(acac)<sub>2</sub> in the hydrothermal reaction. When the molar ratio of Zn and Mn was in the range of 0 to  $1.75 \times 10^{-3}$ ,  $\alpha$ -MnO<sub>2</sub> gradually transformed to  $\beta$ -MnO<sub>2</sub> with an increase in the amount of Zn(acac)<sub>2</sub>. For example,

two phases (34.9% of  $\alpha$ -MnO<sub>2</sub> and 65.1% of  $\beta$ -MnO<sub>2</sub>; Fig. 1B-b) were observed when 3.32 mg of Zn(acac)<sub>2</sub> (Zn/Mn =  $5.0 \times 10^{-4}$ ) was added to the solution. This mixed-phase was assigned  $\alpha$ -MnO<sub>2</sub> and the other tetragonal phase [space group: P42/ mmm (136)] of  $\beta$ -MnO<sub>2</sub> with lattice constants  $a = 4.4071 \text{ \AA}$  and  $c = 2.8740 \text{ \AA}$  (ICSD 98-002-0229). As the amount of Zn(acac)<sub>2</sub> increased to 11.62 mg (Zn/Mn =  $1.75 \times 10^{-3}$ ), only  $\beta$ -MnO<sub>2</sub> was obtained. When the amount of Zn(acac)<sub>2</sub> was increased further,  $\beta$ -MnO<sub>2</sub> disappeared and the original phase ( $\alpha$ -MnO<sub>2</sub>) gradually reappeared. For example, at the Zn/Mn molar ratio of  $2.00 \times 10^{-3}$  (13.28 mg), two phases (14.7 % of  $\alpha$ -MnO<sub>2</sub> and 85.3 % of  $\beta$ -MnO<sub>2</sub>; Fig. 1d) reappeared. Although, when the quantity of Zn(acac)<sub>2</sub> was high up to 255.64 mg (Zn/Mn =  $3.85 \times 10^{-2}$ ), the phase of the sample returned to  $\alpha$ -MnO<sub>2</sub> with the incipient phase, but the crystal was not as perfect as the original  $\alpha$ -MnO<sub>2</sub> due to the presence of Zn species.

The ORR experimental results are shown in the Fig. 2 and Table 1. All the CVs conducted in N<sub>2</sub> did not show any obvious peaks, indicating that no reaction occurred in the N<sub>2</sub>-saturated solution. In contrast, CVs in the O<sub>2</sub>-saturated PBS solution showed distinct oxygen reduction peaks for all the MnO<sub>2</sub> samples. The reduction peaks appeared at more positive potentials (ca. >0.2 V) for all the MnO<sub>2</sub> samples containing  $\beta$ -MnO<sub>2</sub>, while they appeared at a much less positive potential for single-phase  $\alpha$ -MnO<sub>2</sub> samples. Moreover, the results indicate that  $\beta$ -MnO<sub>2</sub> (Zn/Mn =  $1.75 \times 10^{-3}$ ) catalysed ORR at lower overpotentials than the other MnO<sub>2</sub> samples; combined with the observed high peak currents, this shows the superior ORR activities of  $\beta$ -MnO<sub>2</sub> (Zn/Mn =  $1.75 \times 10^{-3}$ ). The preliminary results obtained from this ORR activity study indicate that the ORR activities of MnO<sub>2</sub> samples strongly depend on their crystallographic structures and follow the order:  $\beta$ -MnO<sub>2</sub> (Zn/Mn =  $1.75 \times 10^{-3}$ ) >  $\alpha$ -/ $\beta$ -MnO<sub>2</sub> (Zn/Mn =  $5.0 \times 10^{-4}$ ) >  $\alpha$ -/ $\beta$ -MnO<sub>2</sub> (Zn/Mn =  $2.00 \times 10^{-3}$ ) >  $\beta$ -MnO<sub>2</sub> (commercial) >  $\alpha$ -MnO<sub>2</sub> (Zn/Mn = 0) >  $\alpha$ -MnO<sub>2</sub> (Zn/Mn =  $3.85 \times 10^{-2}$ ).

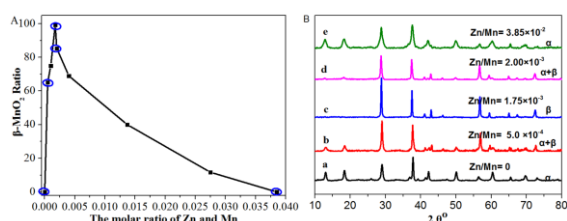


Figure 1. Contents of  $\beta$ -MnO<sub>2</sub> in the mixed-MnO<sub>2</sub> obtained by Rietveld refinement (A), XRD patterns of different compositions of mixed-MnO<sub>2</sub> (B).

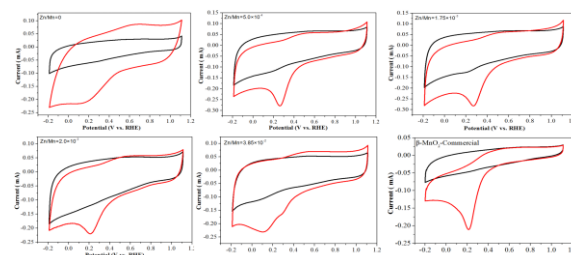


Figure 2. CV curves of different MnO<sub>2</sub> under N<sub>2</sub>-saturated (black line) and O<sub>2</sub>-saturated (red line). 0.1 M PBS aqueous solutions at a scan rate of 100 mV s<sup>-1</sup> between -0.2 and 1.1 V.

Table 1. Summary of the ORR Catalytic Performance Revealed from CV curves

Mix-MnO <sub>2</sub> sample (Zn/Mn atom ratio)	Oxygen reduction potential (V)	Oxygen reduction currents (mA)
0	0.16	-0.21
$5.0 \times 10^{-4}$	0.26	-0.21
$1.75 \times 10^{-3}$	0.27	-0.28
$2.00 \times 10^{-3}$	0.22	-0.22
$3.85 \times 10^{-2}$	0.12	-0.23
$\beta$ -MnO <sub>2</sub> -Commercial	0.21	-0.21

#### 4. Conclusions

In summary, a novel route for the precise-control phase transformation of MnO<sub>2</sub> to synthesise novel  $\alpha$ -/ $\beta$ -MnO<sub>2</sub> materials with different phase compositions by adding a trace amount of Zn(acac)<sub>2</sub> as a PTIA in hydrothermal reactions. The results indicate that the ORR activities of the MnO<sub>2</sub> samples strongly depend on the crystallographic structures and follow the order:  $\beta$ -MnO<sub>2</sub> (Zn/Mn =  $1.75 \times 10^{-3}$ ) >  $\alpha$ -/ $\beta$ -MnO<sub>2</sub> (Zn/Mn =  $5.0 \times 10^{-4}$ ) >  $\alpha$ -/ $\beta$ -MnO<sub>2</sub> (Zn/Mn =  $2.00 \times 10^{-3}$ ) >  $\beta$ -MnO<sub>2</sub> (commercial) >  $\alpha$ -MnO<sub>2</sub> (Zn/Mn = 0) >  $\alpha$ -MnO<sub>2</sub> (Zn/Mn =  $3.85 \times 10^{-2}$ ).

#### References

1. X. F. Shen, Y. S. Ding, J. C. Hanson, M. Aindow and S. L. Suib, J. Am. Chem. Soc. 128 (2006) 4570.
2. X. Wang and Y. Li, J. Am. Chem. Soc., 2002, 124, 2880

Acknowledgements: this work was financially supported by national natural science foundation of China (21777004), the 863 project (2015AA0034603) and General program of science and technology development project of Beijing Municipal Education Commission (KM201810005008).